



OPEN

Effects of transcranial static magnetic stimulation over the primary motor cortex on local and network spontaneous electroencephalogram oscillations

Sumiya Shibata¹✉, Tatsunori Watanabe², Yoshihiro Yukawa³, Masatoshi Minakuchi³, Ryota Shimomura³, Sachimori Ichimura³, Hikari Kirimoto² & Tatsuya Mima⁴✉

Transcranial static magnetic stimulation (tSMS) is a novel non-invasive brain stimulation technique that reduces cortical excitability at the stimulation site. We investigated the effects of tSMS over the left primary motor cortex (M1) for 20 min on the local electroencephalogram (EEG) power spectrum and interregional EEG coupling. Twelve right-handed healthy subjects participated in this crossover, double-blind, sham-controlled study. Resting-state EEG data were recorded for 3 min before the intervention and 17 min after the beginning of the intervention. The power spectrum at the left central electrode (C3) and the weighted phase lag index (wPLI) between C3 and the other electrodes was calculated for theta (4–8 Hz), alpha (8–12 Hz), and beta (12–30 Hz) frequencies. The tSMS significantly increased theta power at C3 and the functional coupling in the theta band between C3 and the parietal midline electrodes. The tSMS over the left M1 for 20 min exhibited modulatory effects on local cortical activity and interregional functional coupling in the theta band. The neural oscillations in the theta band may have an important role in the neurophysiological effects induced by tSMS over the frontal cortex.

Transcranial static magnetic stimulation (tSMS) is a novel non-invasive brain stimulation (NIBS) technique. Through the static magnetic fields (SMFs) produced by a strong, compact neodymium magnet placed on the scalp, tSMS can suppress cortical excitability just below the magnet^{1–4}. Furthermore, we previously reported the modulation of the intracortical excitability in the primary motor cortex (M1) contralateral to the M1 where the magnet is placed⁵. Since tSMS is not associated with induced electric currents, it does not provoke seizures or tingling sensations. Therefore, tSMS is a safe and low-cost technique for neuromodulation.

Investigating changes in spontaneous electroencephalogram (EEG) activity by tSMS is crucial to better understand the neurophysiological effects of tSMS. Rhythmic brain activity is a fundamental property of neural elements and represents the synchronization of oscillations across them⁶. EEG is an electrophysiological technique that noninvasively records the oscillatory characteristics of neuronal activities. It provides a direct index of neuronal functions with high temporal resolution unlike magnetic resonance imaging (MRI), functional MRI, positron emission tomography, and single-photon emission computed tomography. It can also show clear changes in the synchronization within and among neuronal populations in the cerebral cortex. The synchronization evident in EEG can be revealed through spectral analysis⁷. Changes in the synchronization within the local neuronal populations appear as changes in the EEG power spectrum, while those in the synchronization between the neuronal populations appear like those in interregional EEG coupling^{8,9}. Local EEG power spectrum and interregional EEG coupling can be used to assess the neurophysiological effects of tSMS; however, only a limited number of studies have investigated this application^{10–12}.

¹Kinugasa Research Organization, Ritsumeikan University, 56-1, Tojiin, Kitamachi, Kita-ku, Kyoto, Kyoto 603-8577, Japan. ²Department of Sensorimotor Neuroscience, Graduate School of Biomedical and Health Sciences, Hiroshima University, 1-2-3 Kasumi, Minami-ku, Hiroshima, Hiroshima 734-8553, Japan. ³Department of Rehabilitation, Murata Hospital, 4-2-1, Tajima, Ikuno-ku, Osaka, Osaka 544-0011, Japan. ⁴The Graduate School of Core Ethics and Frontier Sciences, Ritsumeikan University, 56-1, Tojiin, Kitamachi, Kita-ku, Kyoto, Kyoto 603-8577, Japan. ✉email: sshiba@kuhp.kyoto-u.ac.jp; t-mima@fc.ritsumei.ac.jp

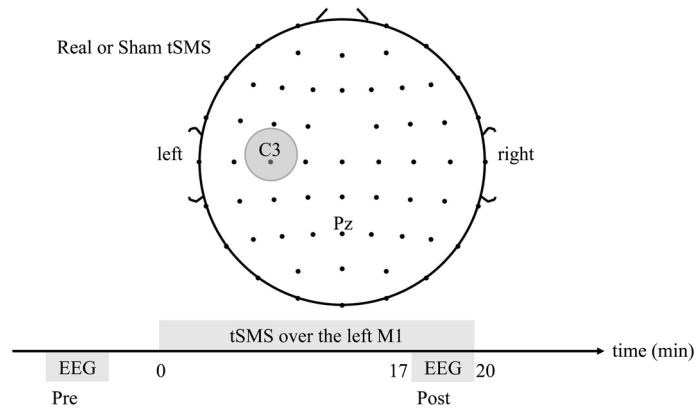


Figure 1. Schematic illustration of the experimental setup. Real or sham tSMS (grey circle) was applied over the left M1 for 20 min. The resting EEG was recorded for 3 min before and during the intervention (Pre and Post respectively).

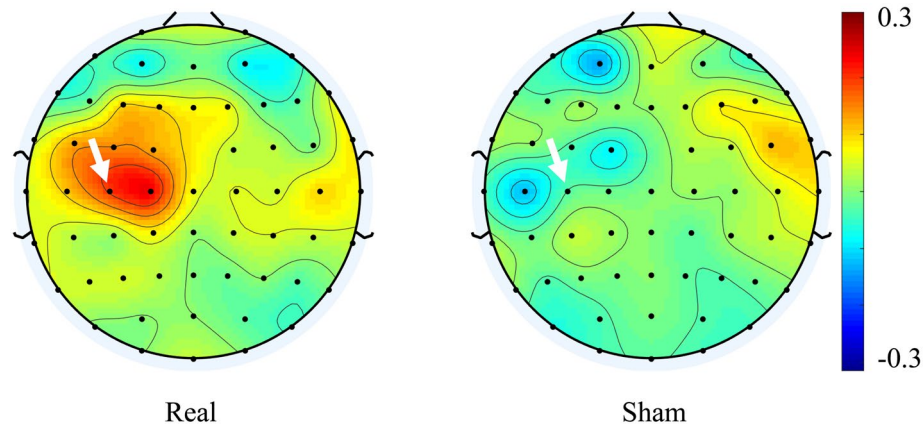


Figure 2. Scalp map of the changes in the EEG power in the theta band averaged across all the subjects for real (left) and sham (right) tSMS. An arrow shows the C3 electrode. Note that the area at C3 was a “hot spot” for real tSMS.

Other NIBS techniques, that inhibit the cortex function at the stimulation site, can modulate synchronization within and among the neuronal populations in the cerebral cortex^{9,13,14}. We hypothesized tSMS to have modulatory effects on both the local EEG power spectrum in the stimulated cortex just below the magnet and the EEG coupling between the stimulated cortex and remote cortex. We conducted a crossover, double-blind, and sham-controlled study to investigate the changes in theta (4–8 Hz), alpha (8–12 Hz), and beta (12–30 Hz) EEG oscillations produced by tSMS. Twelve healthy subjects received real and sham tSMS to their left M1 for 20 min (Fig. 1).

To evaluate the modulation of local cortical activity, the changes in the resting EEG power spectrum at the left central electrode (C3) was compared between the real and sham tSMS. To investigate the modulation of interregional functional coupling, the changes in the weighted phase lag index (wPLI)¹⁵ between C3 and the other electrodes, was compared between the real and sham tSMS. The wPLI is an index of phase-synchronization between two signals. The range of the wPLI is between 0 and 1. Higher wPLI value indicates higher synchronization of the two signals, and vice versa.

Results

Local cortical activity. None of the subjects exhibited any side effects. The changes in the EEG power for the real tSMS and sham tSMS at C3 were 0.20 ± 0.22 and -0.03 ± 0.21 in the theta band, 0.08 ± 0.28 and -0.07 ± 0.23 in the alpha band, and 0.07 ± 0.36 and -0.07 ± 0.30 in the beta band, respectively (the change in the EEG power is a normalized unitless value). Figure 2 shows the changes averaged across all subjects in the theta band for the real and sham tSMS. The area at C3 was a “hot spot” for the real tSMS. The change was significant only in the theta band ($p=0.040$) (Fig. 3). This demonstrates that tSMS could increase the EEG power in the theta band at the stimulation site.

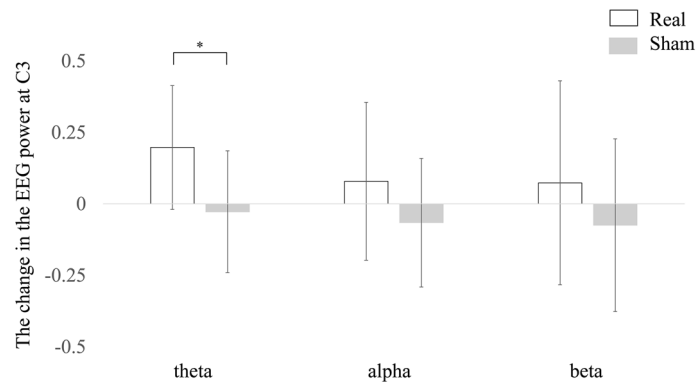


Figure 3. The changes in the EEG power for each frequency band at C3 averaged across all the subjects for the real and sham tSMS. Error bars indicate standard deviation. The change was significant only for the theta band (*).

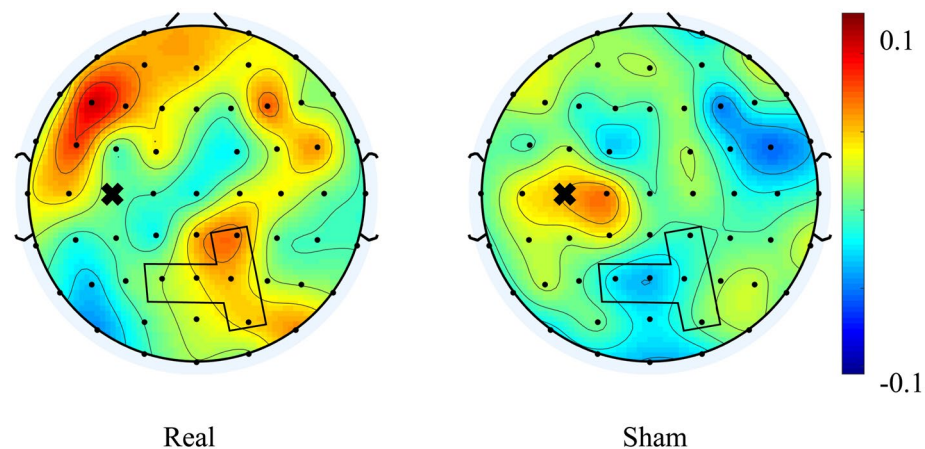


Figure 4. Scalp map of the median across all subjects of the changes in the wPLI in the theta band between C3 and the other electrodes for real (left) and sham (right) tSMS. A cross mark shows the position of C3. The significant cluster was identified at the electrodes surrounded by a black line.

Interregional functional coupling. Supplementary Table S1 shows the changes in the wPLI for each frequency band. The largest cluster of significant electrode pairs were identified as C3-Pz [real: 0.04 (0.02–0.08), sham: -0.04 (-0.13–0.04)], C3-CP2 [real: 0.07 (-0.03–0.14), sham: -0.01 (-0.04–0.03)], C3-P1 [real: 0.02 (-0.02–0.13), sham: -0.03 (-0.05–0.03)], C3-PO4 [real: 0.05 (0.02–0.08), sham: 0.01 (-0.06–0.02)], and C3-P2 [real: 0.05 (-0.01–0.09), sham: -0.01 (-0.10–0.03)] in the theta band. The wPLI before and during the intervention for each frequency band is shown in Supplementary Table S2. Figure 4 shows the spatial distribution of the median across all subjects of the changes in the wPLI in the theta band. TSMS could increase the wPLI between the left central area and the parietal midline.

Discussion

We report that tSMS over the left M1 could increase both the theta EEG power at the stimulation site and functional coupling in the theta band between the stimulation site and the parietal midline. To our knowledge, this is the first study to demonstrate the effects of tSMS on both the local cortical activity and interregional functional coupling.

Regarding the tSMS effect on local cortical activity, previous studies demonstrated that tSMS increased the alpha power on the cortex just below the magnet when applied over the occipital and parietal cortex^{10,11}. These studies suggested that an increase in the local alpha oscillations by tSMS reflect the inhibition of visual¹⁰ and sensory¹¹ functions. However, another study showed that tSMS over the dorsolateral prefrontal cortex (DLPFC) did not change the alpha power at the stimulation site¹². This indicates a location-specific effect of tSMS on local oscillations. In our study, tSMS over the left M1 did not change the alpha power but increased the theta power at the stimulation site. Since tSMS over the DLPFC exhibited a trend-level effect in the theta band¹², the tSMS over the frontal cortex may modulate the theta oscillations.

tSMS over the left M1 increased the functional coupling between the stimulation site and the parietal midline. We previously demonstrated that tSMS over the M1 has a modulatory effect on the contralateral M1⁵. The present study suggests that the interhemispheric effect of tSMS may result from the modulation of the motor network via the parietal area in the theta band. This speculation is compatible with an MRI study showing that the precuneus was connected to areas implicated in motor execution¹⁶.

The results of the present study may partly be explained by the neurophysiological effects of tSMS. Although hippocampal theta rhythms in rodents are established, the theta activity can also be recorded from several extra-hippocampal regions in rodents and humans¹⁷. Generators of theta oscillations are likely located near the surface of the brain and widely distributed over the neocortex¹⁸. Based on the actual measurements of the magnetic field induced by tSMS^{4,19}, tSMS had a sufficient SMF to cause a biological effect on the brain surface (an estimated distance of 2–3 cm from the scalp). Therefore, tSMS can have modulatory effects on the theta oscillations generators near the brain surface. Synchronization of cortical theta oscillations over large regions can cause remote effects of tSMS. Although the neurophysiological mechanisms of the tSMS action on the brain are not yet well defined, previous studies reported that tSMS can modulate the inhibitory systems related to GABA receptor activity^{20,21}. GABAergic neurons or interneurons are likely involved in hippocampal theta oscillations²². The effects of tSMS on theta oscillations may result from the modulation of inhibitory systems related to the GABA receptor activity.

Other NIBS techniques, such as low-frequency repetitive transcranial magnetic stimulation (rTMS) and cathodal transcranial direct current stimulation (tDCS), also inhibit the cortex function at the stimulation site. Variable results exist for the effect of such NIBS techniques on the resting-state EEG power. In healthy humans, low-frequency rTMS (0.9 Hz) over the lateral premotor cortex significantly increased the resting state power in the alpha1 (8–10 Hz) band recorded from the bilateral sensorimotor areas and the mesial frontocentral area, but had no significant effect on the alpha2 (11–13 Hz), beta1 (14–20 Hz) and beta2 (21–30 Hz) bands⁹. In patients suffering from depression, the low-frequency rTMS (1.0 Hz) over the right prefrontal dorsolateral cortex had no significant effect on the resting state power in the delta (1–3.5 Hz), theta (3.5–8 Hz), alpha (8–12 Hz), and beta (12–32 Hz) bands. In healthy humans, the cathodal tDCS over the motor area increased the resting state power in the delta (2–4 Hz) and theta (4–7 Hz) bands¹³. A simultaneous tDCS-EEG study revealed that high-definition cathodal tDCS over the sensorimotor area resulted in a smaller delta (2–4 Hz), theta (4–8 Hz), and alpha (8–13 Hz) response compared to the sham stimulation¹⁴. Although these differences are likely due to differences in the subject population and stimulation, these previous studies demonstrate that NIBS techniques that inhibit brain functions can also modulate spontaneous brain rhythms.

We show that the neural oscillations in the theta band can be modulated by tSMS over the frontal cortex. Based on these findings, tSMS can be used for clinical application in future. Thalamocortical dysrhythmia, which is an abnormally increased thalamocortical activity in the theta band, is likely related to neurological and psychiatric conditions such as neurogenic pain, tinnitus, Parkinson's disease, and depression²³. tSMS may have the potential to modulate such a pathological oscillation in the theta band. Theta activity is also associated with attention and cognitive control in humans and rodents¹⁷. In humans, the sensory, motor, and cognitive functions related to high gamma activities can be coordinated through the theta/high gamma coupling²⁴ indicating that tSMS over the frontal cortex may have behavioral effects through the modulation of theta oscillations. Therefore, tSMS is potentially a safe and low-cost technique for neurological disorders treatment and neurorehabilitation.

The limitation of this study is that EEG does not have a good spatial resolution. Current source density (CSD) estimates through the surface Laplacian computation²⁵, used in this study, improve EEG spatial resolution²⁶. However, the surface-level connectivity data have spurious false positive connections through field spread in the vicinity of true interactions even when using measures that are immune to zero-lag correlations²⁷ such as the wPLI. To avoid neuroanatomical misinterpretations of the coupled sources, it is essential to analyze full source-space interaction mapping. In the cluster-based permutation test for the wPLI, all electrode pairs including C3 were investigated. Considering the result of the cluster-based permutation test for the wPLI, a true interaction was suggested to be localized between the stimulation site and the parietal midline.

In conclusion, we show that tSMS over the left M1 could increase the theta EEG power at the stimulation site and increase the functional coupling in the theta band between the stimulation site and the parietal midline. The oscillatory effects of tSMS may be associated with the modulation of inhibitory systems by the GABA receptor activity. Further studies on the oscillatory effects of tSMS will help elucidate the neurophysiological mechanisms of tSMS.

Methods

Subjects. Twelve healthy subjects (23–34 years of age; mean age \pm standard deviation, 27 ± 3 years; 7 men) were included in this study. Subjects had no history of neurological illness based on self-report. All subjects were right-handed, as determined by the Edinburgh handedness inventory²⁸. The protocol was approved by the Ethics Committees of Ritsumeikan University (Kyoto, Japan) and Murata Hospital (Osaka, Japan). Written informed consent was obtained from all subjects. The study was conducted according to the Declaration of Helsinki.

Transcranial static magnetic stimulation. A cylindrical nickel-plated (Ni–Cu–Ni) NdFeB magnet with a 50 mm diameter and 30 mm thickness (Model N-50; NeoMag, Chiba, Japan) was used for tSMS. The maximum energy density was 406 kJ/m^3 , with a nominal strength of 863 N. The surface magnetic flux density was approximately 5340 G^5 . A non-magnetic stainless-steel cylinder of similar size and appearance to the real magnet was used for the sham stimulation. The magnet and the non-magnetic cylinder were set using an arm-type light stand (C-stand; Avenger, Cassola, Italy) over the representational area for the right first dorsal interosseous (FDI) muscle (the left M1). They were electrically isolated from EEG electrodes. The left M1 (coil position which led to the largest motor evoked potentials of FDI) was identified by TMS (Magstim 200 magnetic stimulator;

Magstim Co., Whitland, UK). The magnet was held tangentially against the subject's head and the intervention duration was set to 20 min, as with previous studies^{5,20}.

Experimental procedure. Subjects were seated on a chair under normal room light during the experiment. Each subject received both the real and sham tSMS on different days. To avoid the carryover effects³, the interval between the real and sham tSMS was set to be more than 3 days. The stimulation performed on the first day was randomly assigned to the subjects; they were blinded to the type of stimulation. EEG data were recorded using a 64-channel electrode cap (EASYCAP, Herrsching, Germany) with electrodes and an EEG amplifier (Brain Products, Gilching, Germany), at a sampling rate of 5 kHz and a 1350 Hz anti-aliasing filter. FCz and AFz were used as the reference and ground, respectively. We maintained an impedance of less than 10 k Ω for each electrode.

Before the intervention, the resting-state EEG data were recorded for 3 min with the eyes open (Pre). The magnet or the sham device was placed on the EEG cap, just above the left M1. Resting-state EEG data were recorded for 3 min with the eyes open 17 min after the beginning of the intervention (Post). During the EEG recordings (Pre and Post), subjects were instructed to fixate on a crosshair at the center of the display, placed 1 m in front of them. The subjects were acoustically isolated through continuous pink noise provided via insert earphones. The testing was performed in a double-blinded manner: Investigator 1 selected and placed the real magnet or sham stainless-steel cylinder, and Investigator 2, who was blinded to the type of intervention being performed, recorded EEGs and analyzed them.

EEG and statistical analyses. EEG and statistical analyses were performed using EEGLAB²⁹, MATLAB (MathWorks Inc., Natick, MA, USA), Excel (Microsoft Inc., Redmond, WA, USA), and SPSS (SPSS Inc., Chicago, IL, USA). Data were down-sampled to 1 kHz and filtered from 1 to 50 Hz. Bad channels were identified through visual inspection and were removed and interpolated. After re-referencing to the common average, data were epoched into 2 s windows. The epochs were visually inspected and the bad epochs containing large artifacts were removed. Independent component analysis (ICA) was conducted using MARA³⁰ to remove any remaining artifacts. The resulting data were then converted to CSD²⁵ to increase the spatial selectivity.

The theta, alpha, and beta components were obtained by applying the band-pass filters of 4–8, 8–12, and 12–30 Hz to each of the 2 s epoch, respectively. A Hilbert transformation was applied to the filtered signals. To evaluate the effect of tSMS on the EEG power in the cortex just below the magnet, the power spectrum at C3 was analyzed. The EEG activity at C3 represents the primary sensorimotor cortex activity³¹. To evaluate the effect of tSMS on the connectivity between the cortex, just below the magnet, and other areas, the wPLI between C3 and the other electrodes was calculated for each frequency band. The temporal power/wPLI data were calculated for each time point and averaged across all time points over all epochs.

For statistical analysis, the change in the EEG power was computed according to the formula: the change in the EEG power = \log_{10} (the EEG power at Post / the EEG power at Pre) (the change in the EEG power is a normalized unitless value). Once the normal distribution was confirmed for the change in the EEG power using the Shapiro–Wilk test ($p = 0.416$), it was compared between the two conditions (real and sham tSMS) using Student's paired-samples t-test. The result was considered statistically significant at $p < 0.05$.

A non-parametric cluster-based permutation test³² was conducted for the analysis of the wPLI between C3 and the other electrodes. The change in the wPLI was computed as the wPLI at Post—the wPLI at Pre. T-values are calculated between the two stimulations for each electrode pair for each frequency band, and 1000 permutations of the two stimulations for each subject were performed to create a distribution of the t-values for each electrode pair for each frequency band. If the original t-value was at the 97.5th percentile on either tail, the electrode pair was considered as significant. If the counterpart electrodes of C3 in two significant electrode pairs were nearest-neighbor (adjacent) electrodes, these electrode pairs were identified as a cluster. The cluster including the largest number of adjacent counterpart electrodes through the three frequency bands was considered as a significant cluster. Values reported in the text are mean \pm standard deviation or median (interquartile range).

Data availability

The datasets generated and/or analyzed during the current study are available from a corresponding author upon reasonable request.

Received: 4 December 2020; Accepted: 22 March 2021

Published online: 15 April 2021

References

- Oliviero, A. *et al.* Transcranial static magnetic field stimulation of the human motor cortex. *J. Physiol.* **589**, 4949–4958. <https://doi.org/10.1113/jphysiol.2011.211953> (2011).
- Silbert, B. I., Pevcic, D. D., Patterson, H. I., Windnagel, K. A. & Thickbroom, G. W. Inverse correlation between resting motor threshold and corticomotor excitability after static magnetic stimulation of human motor cortex. *Brain Stimul.* **6**, 817–820. <https://doi.org/10.1016/j.brs.2013.03.007> (2013).
- Kirimoto, H. *et al.* Effect of transcranial static magnetic field stimulation over the sensorimotor cortex on somatosensory evoked potentials in humans. *Brain Stimul.* **7**, 836–840. <https://doi.org/10.1016/j.brs.2014.09.016> (2014).
- Kirimoto, H., Asao, A., Tamaki, H. & Onishi, H. Non-invasive modulation of somatosensory evoked potentials by the application of static magnetic fields over the primary and supplementary motor cortices. *Sci. Rep.* **6**, 34509. <https://doi.org/10.1038/srep34509> (2016).
- Shibata, S. *et al.* Effect of transcranial static magnetic stimulation on intracortical excitability in the contralateral primary motor cortex. *Neurosci. Lett.* **723**, 134871. <https://doi.org/10.1016/j.neulet.2020.134871> (2020).

6. Thut, G. & Miniussi, C. New insights into rhythmic brain activity from TMS–EEG studies. *Trends Cognit. Sci.* **13**, 182–189. <https://doi.org/10.1016/j.tics.2009.01.004> (2009).
7. Pfurtscheller, G. & Da Silva, F. L. Event-related EEG/MEG synchronization and desynchronization: basic principles. *Clin. Neurophysiol.* **110**, 1842–1857. [https://doi.org/10.1016/s1388-2457\(99\)00141-8](https://doi.org/10.1016/s1388-2457(99)00141-8) (1999).
8. Andres, F. G. *et al.* Functional coupling of human cortical sensorimotor areas during bimanual skill acquisition. *Brain* **122**, 855–870. <https://doi.org/10.1093/brain/122.5.855> (1999).
9. Chen, W. H. *et al.* Low-frequency rTMS over lateral premotor cortex induces lasting changes in regional activation and functional coupling of cortical motor areas. *Clin. Neurophysiol.* **114**, 1628–1637. [https://doi.org/10.1016/s1388-2457\(03\)00063-4](https://doi.org/10.1016/s1388-2457(03)00063-4) (2003).
10. Gonzalez-Rosa, J. J. *et al.* Static magnetic field stimulation over the visual cortex increases alpha oscillations and slows visual search in humans. *J. Neurosci.* **35**, 9182–9193. <https://doi.org/10.1523/JNEUROSCI.4232-14.2015> (2015).
11. Carrasco-López, C. *et al.* Static magnetic field stimulation over parietal cortex enhances somatosensory detection in humans. *J. Neurosci.* **37**, 3840–3847 (2017).
12. Sheffield, A., Ahn, S., Alagapan, S. & Fröhlich, F. Modulating neural oscillations by transcranial static magnetic field stimulation of the dorsolateral prefrontal cortex: a crossover, double-blind, sham-controlled pilot study. *Eur. J. Neurosci.* **49**, 250–262. <https://doi.org/10.1111/ejn.14232> (2019).
13. Ardolino, G., Bossi, B., Barbieri, S. & Priori, A. Non-synaptic mechanisms underlie the after-effects of cathodal transcutaneous direct current stimulation of the human brain. *J. Physiol.* **568**, 653–663. <https://doi.org/10.1113/jphysiol.2005.088310> (2005).
14. Roy, A., Baxter, B. & He, B. High-definition transcranial direct current stimulation induces both acute and persistent changes in broadband cortical synchronization: a simultaneous tDCS–EEG study. *IEEE Trans. Biomed. Eng.* **61**, 1967–1978. <https://doi.org/10.1109/Tbme.2014.2311071> (2014).
15. Vinck, M., Oostenveld, R., Van Wingerden, M., Battaglia, F. & Pennartz, C. M. An improved index of phase-synchronization for electrophysiological data in the presence of volume-conduction, noise and sample-size bias. *Neuroimage* **55**, 1548–1565. <https://doi.org/10.1016/j.neuroimage.2011.01.055> (2011).
16. Zhang, S. & Chiang-shan, R. L. Functional connectivity mapping of the human precuneus by resting state fMRI. *Neuroimage* **59**, 3548–3562. <https://doi.org/10.1016/j.neuroimage.2011.11.023> (2012).
17. Kahana, M. J., Seelig, D. & Madsen, J. R. Theta returns. *Curr. Opin. Neurobiol.* **11**, 739–744. [https://doi.org/10.1016/s0959-4388\(01\)00278-1](https://doi.org/10.1016/s0959-4388(01)00278-1) (2001).
18. Noh, N. A., Fuggetta, G., Manganotti, P. & Fiaschi, A. Long lasting modulation of cortical oscillations after continuous theta burst transcranial magnetic stimulation. *PLoS ONE* **7**, e35080. <https://doi.org/10.1371/journal.pone.0035080> (2012).
19. Rivadulla, C., Foffani, G. & Oliviero, A. Magnetic field strength and reproducibility of neodymium magnets useful for transcranial static magnetic field stimulation of the human cortex. *Neuromodul. J. Int. Neuromodul. Soc.* **17**, 438–442. <https://doi.org/10.1111/ner.12125> (2014).
20. Nojima, I., Koganemaru, S., Fukuyama, H. & Mima, T. Static magnetic field can transiently alter the human intracortical inhibitory system. *Clin. Neurophysiol.* **126**, 2314–2319. <https://doi.org/10.1016/j.clinph.2015.01.030> (2015).
21. Dileone, M., Mordillo-Mateos, L., Oliviero, A. & Foffani, G. Long-lasting effects of transcranial static magnetic field stimulation on motor cortex excitability. *Brain Stimul.* **11**, 676–688. <https://doi.org/10.1016/j.brs.2018.02.005> (2018).
22. Buzsáki, G. Theta oscillations in the hippocampus. *Neuron* **33**, 325–340 (2002).
23. Llinas, R. R., Ribary, U., Jeanmonod, D., Kronberg, E. & Mitra, P. P. Thalamocortical dysrhythmia: a neurological and neuropsychiatric syndrome characterized by magnetoencephalography. *Proc. Natl. Acad. Sci. U.S.A.* **96**, 15222–15227. <https://doi.org/10.1073/pnas.96.26.15222> (1999).
24. Canolty, R. T. *et al.* High gamma power is phase-locked to theta oscillations in human neocortex. *Science* **313**, 1626–1628. <https://doi.org/10.1126/science.1128115> (2006).
25. Kayser, J. & Tenke, C. E. Principal components analysis of Laplacian waveforms as a generic method for identifying ERP generator patterns: I. Evaluation with auditory oddball tasks. *Clin. Neurophysiol.* **117**, 348–368. <https://doi.org/10.1016/j.clinph.2005.08.034> (2006).
26. Burle, B. *et al.* Spatial and temporal resolutions of EEG: is it really black and white? A scalp current density view. *Int. J. Psychophysiol.* **97**, 210–220. <https://doi.org/10.1016/j.ijpsycho.2015.05.004> (2015).
27. Palva, J. M. *et al.* Ghost interactions in MEG/EEG source space: a note of caution on inter-areal coupling measures. *Neuroimage* **173**, 632–643. <https://doi.org/10.1016/j.neuroimage.2018.02.032> (2018).
28. Oldfield, R. C. The assessment and analysis of handedness: the Edinburgh inventory. *Neuropsychologia* **9**, 97–113. [https://doi.org/10.1016/0028-3932\(71\)90067-4](https://doi.org/10.1016/0028-3932(71)90067-4) (1971).
29. Delorme, A. & Makeig, S. EEGLAB: an open source toolbox for analysis of single-trial EEG dynamics including independent component analysis. *J. Neurosci. Methods* **134**, 9–21. <https://doi.org/10.1016/j.jneumeth.2003.10.009> (2004).
30. Winkler, I., Haufe, S. & Tangermann, M. Automatic classification of artifactual ICA-components for artifact removal in EEG signals. *Behav. Brain Funct.* **7**, 30. <https://doi.org/10.1186/1744-9081-7-30> (2011).
31. Mima, T., Simpkins, N., Oluwatimilehin, T. & Hallett, M. Force level modulates human cortical oscillatory activities. *Neurosci. Lett.* **275**, 77–80. [https://doi.org/10.1016/s0304-3940\(99\)00734-x](https://doi.org/10.1016/s0304-3940(99)00734-x) (1999).
32. Maris, E. & Oostenveld, R. Nonparametric statistical testing of EEG- and MEG-data. *J. Neurosci. Methods* **164**, 177–190. <https://doi.org/10.1016/j.jneumeth.2007.03.024> (2007).

Acknowledgements

This study was supported by Grants-in-Aid for Scientific Research (KAKENHI) [grant number 15H05880 (TM), 19H01091 (TM), and 19K24329 (SS)] from the Japan Society for the Promotion of Science. We thank Dr. Takaho Murata and Dr. Daiki Murata at Murata Hospital for their support.

Author contributions

S.S., T.W., and T.M. conceived the study and designed the experimental paradigm. S.S., T.W., Y.Y., M.M., R.S., and S.I. performed the experiment. S.S. and T.M. analyzed the data. S.S. wrote the manuscript. T.W., H.K., and T.M. provided feedback and edited the manuscript. All authors have read and approved the final manuscript.

Competing interests

The authors declare no competing interests.

Additional information

Supplementary Information The online version contains supplementary material available at <https://doi.org/10.1038/s41598-021-87746-2>.

Correspondence and requests for materials should be addressed to S.S. or T.M.

Reprints and permissions information is available at www.nature.com/reprints.

Publisher's note Springer Nature remains neutral with regard to jurisdictional claims in published maps and institutional affiliations.



Open Access This article is licensed under a Creative Commons Attribution 4.0 International License, which permits use, sharing, adaptation, distribution and reproduction in any medium or format, as long as you give appropriate credit to the original author(s) and the source, provide a link to the Creative Commons licence, and indicate if changes were made. The images or other third party material in this article are included in the article's Creative Commons licence, unless indicated otherwise in a credit line to the material. If material is not included in the article's Creative Commons licence and your intended use is not permitted by statutory regulation or exceeds the permitted use, you will need to obtain permission directly from the copyright holder. To view a copy of this licence, visit <http://creativecommons.org/licenses/by/4.0/>.

© The Author(s) 2021